Ecotoxicology and Environmental Safety 215 (2021) 112108

Contents lists available at ScienceDirect

Ecotoxicology and Environmental Safety

journal homepage: www.elsevier.com/locate/ecoenv

Probiotic alleviate fluoride-induced memory impairment by reconstructing gut microbiota in mice

Jinge Xin [a,1], Hesong Wang [b,1], Ning Sun [a], Shamsuddin Bughio [c], Dong Zeng [a], Lianxin Li [a], Yanyan Wang [a], Abdul Khalique [a], Yan Zeng [a], Kangcheng Pan [a], Bo Jing [a], Hailin Ma [d,e], Yang Bai [b,*], Xueqin Ni [a,**]

[a] Animal Microecology Institute, College of Veterinary Medicine, Sichuan Agricultural University, Chengdu, Sichuan, China
[b] Guangdong Provincial Key Laboratory of Gastroenterology, Department of Gastroenterology, Institute of Gastroenterology of Guangdong Province, Nanfang Hospital, Southern Medical University, Guangzhou, China
[c] Department of Veterinary Pharmacology, Sindh Agriculture University Tandojam, Pakistan
[d] Plateau Brain Science Research Center, South China Normal University, Guangzhou 510631, China
[e] Tibet University, Lhasa 850012, China

ARTICLE INFO

Edited by: Professor Bing Yan

Keywords:
Fluoride
Lactobacillus johnsonii BS15
Memory dysfunction
Gut–brain axis
Hippocampus
Gut microbiota

ABSTRACT

Fluoride which is widespread in our environment and food due to its geological origin and industrial pollution has been identified as a developmental neurotoxicant. Gut-brain axis provides new insight into brain-derived injury. We previously found the psychoactive effects of a probiotic strain, *Lactobacillus johnsonii* BS15 against fluoride-induced memory dysfunction in mice by modulating the gut-brain axis. In this study, we aimed to detect the link between the reconstruction of gut microbiota and gut-brain axis through which probiotic alleviate fluoride-induced memory impairment. We also added an hour of water avoidance stress (WAS) before behavioral tests and sampling, aiming to demonstrate the preventive effects of the probiotic on fluoride-induced memory impairment after psychological stress. Mice were given fluoridated drinking water (sodium fluoride 100 ppm, corresponding to 37.8 ± 2.4 ppm F^-) for 70 days and administered with PBS or a probiotic strain, *Lactobacillus johnsonii* BS15 for 28 days prior to and throughout a 70 day exposure to sodium fluoride. Results showed that fluoride increases the hyperactivity of hypothalamic-pituitary-adrenal (HPA) axis and reduces the exploration ratio in novel object recognition (NOR) test and the spontaneous exploration during the T-maze test in mice following WAS, which were significantly improved by the probiotic. 16S rRNA sequencing showed a significant separation in ileal microbiota between the fluoride-treated mice and control mice. *Lactobacillus* was the main targeting bacteria and significantly reduced in fluoride-treated mice. BS15 reconstructed the fluoride-post microbiota and increased the relative abundance of *Lactobacillus*. D-lactate content and diamine oxidase (DAO) activity, two biomarkers of gut permeability were reduced in the serum of probiotic-inoculated mice. ZO-1, an intestinal tight junction protein was reduced by fluoride in mRNA, and its protein levels were increased by the probiotic treatment. Moreover, the hippocampus which is essential to learning and memory, down-regulated mRNA level of both the myelin-associated glycoprotein (MAG), and protein levels of brain-derived neurotrophic factor (BDNF), including the improvement of cAMP response element-binding protein (CREB) by BS15 in fluoride-exposed mice after WAS. Via spearman correlation analysis, *Lactobacillus* displayed significantly positive associations with the behavioral tests, levels of nerve development related factors, and intestinal tight junction proteins ZO-1, and negative association with TNF-α of the hippocampus, highlighting regulatory effects of gut bacteria on memory potential and gut barrier. These results suggested the psychoactive effects of BS15 on fluoride-induced memory dysfunction after psychological stress. In addition, there may be some correlations between fluoride-induced memory dysfunction and reconstruction of gut microbiota.

* Correspondence to: 1838 Guangzhou Avenue, Guangzhou 510000, Guangdong, China.
** Correspondence to: 211 Huimin Road, Chengdu 610400, Sichuan, China.
E-mail addresses: 13925001665@163.com (Y. Bai), xueqinni@foxmail.com (X. Ni).
[1] These authors are equal contributors.

https://doi.org/10.1016/j.ecoenv.2021.112108
Received 10 October 2020; Received in revised form 23 February 2021; Accepted 24 February 2021
Available online 30 March 2021

Availability of data and materials: 16S rRNA sequencing reads have uploaded to NCBI. The accession code of 16S rRNA sequencing reads in the National Center for Biotechnology Information (NCBI) BioProject database: PRJNA660154.

1. Introduction

Fluoride is a widespread environmental pollution, and groundwater is the major source of exposure in which the fluoride concentration can be as high as 35 ppm (Petrone et al., 2013). Fluorosis induced by geological origin is a serious public health concern in 28 nations particularly in India and China (Rafique et al., 2015). In India, 230 districts of 20 states are at risk of a high level of fluoride in drinking water (Srivastava and Flora, 2020). In China, almost all the provinces have reported fluorosis except for Shanghai and Hainan (Sun, 2010; Sun et al., 2009). Moreover, social modernization results in fluoride pollution because of industrial production, the mechanical processing of food, and the use of fluorine-containing crop protection. Based on previous reports, fluoride concentration in canned meat and brick tea is under 1 to more than 8.6 mg/kg (Fein and Cerklewski, 2001) and 600–2800 mg/kg (Fung et al., 1999), respectively. Fluoride accumulation in our body can damage both bone (Petrone et al., 2013) and non-bone tissues (Yan et al., 2019; Qian et al., 2013), such as the liver, kidney, spleen, and brain. The neurotoxic effects of fluorine must not be ignored because such effects can affect brain health in rodents at levels below those that induce dental lesions (Grandjean, 2019). To date, fluoride has been identified as a developmental neurotoxicant (Grandjean and Landrigan, 2014).

Recently, there is increasing evidence on fluoride-induced brain damage by focusing on learning and memory dysfunction. An epidemiological study from Hulunbuir, Inner Mongolia of China based on 331 children aged 7–14 from four schools with the same teaching quality demonstrated that fluoride exposure even in low levels had negative effects on children's memory (Ding et al., 2011). Similar studies were also found in other countries (Green et al., 2020; Bashash et al., 2017). Moreover, Liu et al. (2010) found that a rat exposed to fluoride (50 ppm NaF) for 6 months showed prolonged escape latency in the Morris water maze test. Other rodent experiments also demonstrated that fluoride exposure could cause microtubule lesions; thickened postsynaptic density; pathologic, indistinct, and short synaptic cleft; and myelin damage (Niu et al., 2018). Furthermore, brain-derived neurotrophic factor (BDNF) and cAMP/Ca^{2+}-responsive element-binding protein (CREB), which have been identified to be involved in hippocampal plasticity and hippocampus-dependent memory based on considerable evidence, were decreased in mice exposed to fluoride (100 ppm NaF) for 60 days (Niu et al., 2018).

Moreover, fluoride-exposed mice were not only confronted by memory impairment but also accompanied by intestinal inflammation and increased gut permeability. It is well accepted that intestinal microbiota highly shapes the intestinal microenvironment including intestinal barrier function and intestinal inflammation (Xin et al., 2020). Interestingly, increasing evidence has demonstrated that the gut microbiota is associated with mood and memory disturbances, and improving the gut microbiota is a potential method to treat such diseases. For example, patients with colitis characterized by disordered gut microbiota have a high risk for anxiety (21%) and depression (15%) (Neuendorf et al., 2016). Different colitis models represent the human behavioral phenotype. Zhao et al. (2020) found that the depression and anxiety-like behavior in dextran sulfate sodium-induced colitis model could be improved by lycopene through increasing the relative abundance of *Bifidobacterium* and *Lactobacillus*. Similarly, Jang et al. (2018) inoculated *Lactobacillus johnsonii* to 2,4,6-trinitrobenzenesulfonic acid-induced colitis model, which improved memory impairment by restoring the disturbed gut microbiota composition. Neuroactive metabolites and gut integrity are the main mechanisms underlying the communication between the gut and brain. Recently, Mao et al. (2020) observed increased levels of lactate in the fecal and brains of mice inoculated with *Lactobacillus*, and consequently, the mice had an improved memory. High levels of GABA are linked to novel object recognition and improved working memory and are consumed and produced by the gut microbiota, which influences circulating GABA levels (Strandwitz, 2018). Damage to gut integrity can cause bacteria and harmful metabolites to enter the brain. Recently, Emery et al. (2017) found evidence for microbiological incursion into the brain. Zhan et al. (2016) found increased levels of *Escherichia coli* K99 and lipopolysaccharide (LPS) in Alzheimer's disease (AD) brain and suggested that Gram-negative bacteria-derived LPS induced AD neuropathology in an ischemia–hypoxia rat model. Collectively, these studies indicate a link between the gut microbiota and memory potential.

Luo et al. (2016) found that *Lactobacillus* spp. remarkably decreased and *E. coli* and *Enterococcus* spp. increased in fluoride-treated broiler. Thus, studies based on gut-brain axis hypothesis may be effective in preventing the fluoride-associated memory impairment through the modulation of gut environment by probiotics. *Lactobacillus. johnsonii* BS15 (CCTTCC M2013663) was isolated from homemade yogurt collected from Hongyuan Prairie, Aba Autonomous Prefecture, China. L. *johnsonii* BS15 showed a steady effect on adjusting the gut environment and lowering the intestinal permeability of mice with high-fat diet, thereby preventing non-alcoholic fatty liver disease (Xin et al., 2014). L. *johnsonii* BS15 could also be considered as a potential "psychobiotic" as it was found to prevent psychological stress-induced memory dysfunction in mice by modulating the gut environment (Wang et al., 2020). Therefore, we selected L. *johnsonii* BS15 to regulate the gut environment, aiming to demonstrate the relationship between the intestinal environment and the memory impairment in fluoride-exposed mice. The psychoactive effect of L. *johnsonii* BS15 against fluoride-exposed memory dysfunction through gut-brain axis was revealed in our previous study (Xin et al., 2020). However, to further understand the mechanism underlying the psychoactive effect, it is still important to establish the microbiome-gut-brain axis by detecting the reconstruction of gut microbiota. Though the underlying mechanism remains elusive, a close relationship between psychological stress and intestinal inflammation has been widely accepted (Wu et al., 2014). Moreover, according to our previous study, memory dysfunction was found in mice subjected to 7-day water-avoidance stress (WAS), and the gut-brain axis was also significantly influenced (Wang et al., 2020). As part of our project to demonstrate the mechanism of fluoride-induced memory dysfunction and the effects of modulating gut-brain axis, we were also interested in determining whether or not the probiotic could alleviate fluoride-induced memory impairment after psychological stress.

Therefore, we used 16S rRNA gene sequencing to detect the feature of the gut microbiota in fluoride-treated mice and BS15-treated mice in the present study. In addition, we assessed the difference in memory ability between untreated and treated individuals by T-maze test and novel object recognition (NOR) test after psychological stress. We selected 1 h of WAS as the psychological stress since a single 1 h of WAS did not result in a measurable change in memory ability but might aggravate the memory impairment when other stressor was given (Gareau et al., 2011). In addition to evaluating the intestinal integrity and permeability, hippocampal inflammation and memory-associated protein were detected in this study given the importance of the hippocampus on memory function. The present study aimed to provide evidence to answer the following two research questions: 1) Was the gut microbiota reconstructed by L. *johnsonii* BS15 when using the probiotic to modulate the gut-brain axis and alleviate fluoride-induced memory

impairment? 2) Did the preventive effects of L. *johnsonii* BS15 still exist on fluoride-induced memory impairment after psychological stress?

2. Materials and Methods

2.1. Culture and treatment with BS15

L. *johnsonii* BS15 was grown under anaerobic condition in de Man–Rogosa–Sharpe broth (Qingdao Rishui Bio-technologies Co., Ltd., Qingdao, China) at 37 °C for 24 h. The number of bacterial cells was assessed by heterotrophic plate counts. L. *johnsonii* BS15 cells were then centrifuged (10,000×g, 10 min at 4 °C), washed three times by phosphate-buffered saline (PBS), and re-suspended in PBS (pH 7.0) at a density of 1×10^9 cfu cells/mL (daily consumption dose: 0.2 mL/mice). L. *johnsonii* BS15 was gavaged to mice once a day at 9:00 am.

2.2. Water avoidance stress (WAS)

Water avoidance stress, a well-established model of psychological stress in mice, was used in our study as a psychological stressor. Mice were exposed to WAS, as Gareau et al. (2011) described with minor modifications. In brief, mice were placed on a small platform surrounded by room-temperature water (1 cm below the platform) in the middle of the home cage for 1 h. All the WAS and behavioral tests were carried out between 7:00 am–11:30 am. The schematic outline of WAS was shown in Fig. A.1A (Supplementary materials).

2.3. Behavioural tests

Two observers simultaneously recorded the results of the T-maze and NOR tests to eliminate the influence of concentration loss. Observers were blind to the treatment conditions of each mice and remained unchanged in the same behavioural test.

NOR test: The novel object recognition test was used to assess the ability of rodents to recognize a novel object in the environment. It is a widely used method for the detection of working memory alterations based on nature propensity for novel objects displayed by rodents. In the NOR test, memory formation mainly depends on dorsal hippocampus which plays an important role, especially when spatial or contextual information is a relevant factor (Goulart et al., 2010). The task procedure included three phases (Antunes and Biala, 2012): habituation, familiarization, and test phase. Schematic outline of NOR test was displayed in Fig. A.1C (Supplementary materials). In brief, in the habituation phase, each mouse was placed into the empty open-field arena (l × b × h = 40 cm × 40 cm × 45 cm) for 1 h for habituation. The mouse was then removed from the arena and placed in its home cage. During the familiarization phase, one mouse, following 1 h WAS, was placed in the arena containing two different objects (#A+#B) for 5 min. These two objects were placed in opposite corners of the cage. Then, the mouse was removed from the arena and returned to its cage for a 20 min rest. During the test phase, the mouse was returned to the arena and confronted with object B and a novel object (object #C, distinguishable from object #A). Exploration ratio (F#C/(F#C + F#B) × 100, F#C = frequency of exploring the object #C, F#B = frequency of exploring the object #B), which was used to assess the memory, was calculated.

The tendency of mice to explore novelty indicated that the presentation of the familiar object existed in their memory. The objects used included a green bottle cap (#A), an orange bottle cap (#B), and a small smooth stone (#C). To avoid object bias, our preliminary studies revealed that mice showed equal preference for #A, #B and #C.

T-Maze test: T-maze alternation has been used for decades in academia and industry for its sensitivity in assessing cognitive dysfunction and its simplicity of construction (Deacon and Rawlins, 2006). Spontaneous alternation of T-maze task relies on the novelty of the maze and does not need food restriction. Mice with removed or damaged (e.g., by surgical removal or genetic modification) hippocampus can generally solve very difficult reference memory problems, as long as there is no spatial component (Deacon and Rawlins, 2006). T-maze test which represents spatial working memory makes up for it (Deacon and Rawlins, 2006). Enclosed T-maze, an apparatus with 10 cm-wide floor and 20 cm-high walls in the form of a "T" placed horizontally, was used. The stem of the two goal arms and a start arm was all 30 cm long. A central partition was placed in the middle of two goal arms extending into the start arm (7 cm). Every arm had a guillotine door. Schematic outline of T-maze apparatus was displayed in Fig. A.1B (Supplementary materials). The apparatus and operating steps were consistent with Deacon and Rawlins (2006). First, the central partition was placed in the T-maze with all the doors open. Then, the mouse, directly from its home cage or flowing exposure to WAS, was placed in the start area and allowed to select the left or right arm. The mouse was kept in the chosen arm by quietly sliding the door down. After 30 s, the mouse and central partition were removed, and the mouse was returned to its holding cage. After a retention interval of 1 min, the mouse was placed in the start area for a second trial with all the doors open. There is no habituation to the maze during spontaneous alternation due to the novelty of the maze is involved to drive the spontaneous alternation (Deacon and Rawlins, 2006). To avoid that the mouse felt sated with exploring the maze, each rodent was tested for 5 days with two trials per day. If the mouse selected the other goal arm in consecutive trials, then this trial was marked as "correct." Each exploration should take no more than 2 min. If one mouse fails to run within 90 s, a reasonable criterion at which to abort the trial, it was removed and tested again after resting (Deacon and Rawlins, 2006).

2.4. Establishment of an animal model and study design

A total of 108 male ICR mice (3 weeks old, Chengdu Dashuo Biological Institute, Chengdu, China) were given 1 week to adapt to the new environment. After the adaptation period, mice were randomly divided into three groups and administered with either PBS (control group, F group) or L. *johnsonii* BS15 (prob group; 0.2 mL/day) for 28 days prior to and throughout a 70 day exposure to sodium fluoride. Mice were provided fluoridated drinking water (100 ppm NaF; corresponding to 37.8 ± 2.4 ppm F^-) from 28 days to 98 days, except for the control group. The method of actual concentration detection of sodium fluoride in drinking water can be found in supplementary (Supplementary Note 1). The selection of fluoride dose was based on (i) documented human exposures (The range of fluoride dose in adult is 0.84–27.1 mg per day, 0.19–6.02 ppm when converted to ppm [based on a 55 kg person drinking 4.5 L of water per day]; Supplementary Note 2 and Table A.1), (ii) a dose equivalent equation adjusting for surface area differences between mice and humans (Coryell et al., 2018) (Supplementary Note 2), (iii) the use of similar exposures in studies researching fluoride-associated brain lesion in mice (Table A.2), and (iv) high dose for the potential damage in a shortened test period. Mice were housed in a constant-temperature (20–22 °C) room with a 12 h light/dark cycle (lights on from 06:00 to 18:00) and given free access to water and normal chow diet (Chengdu Dashuo Biological Institute). Each group contains six cages with six individuals per cage. All animal experiments were performed according to the guidelines for the care and use of laboratory animals approved by the Institutional Animal Care and Use Committee of Sichuan Agricultural University (approval number: SYXKchuan2019-187). At the end of the experiment, ten mice (one or two mice per cage) from each group were used for behavioral testing. Another twenty mice in each group were used for sampling. The extra mice were kept on feeding until they die.

2.5. Biochemical evaluation

On day 98 of the experiment, six mice (one mouse per cage) from the control, F, and prob groups were selected and sacrificed by cervical dislocation for sampling following exposure to 1 h WAS. Blood was sampled from the mice orbit, and serum was separated by incubation at

4 °C for 30 min, followed by centrifugation at 2000 × g for 20 min, and stored at − 30 °C. The ileal tissue and right hippocampus were ground (pH 7.4) into 10% or 5% homogenate with PBS, respectively, and then centrifuged (12,000 × g for 5 min at 4 °C). The obtained liquid supernatant was used for biochemical detection. The D-lactate and diamine oxidase (DAO) activity, contents of corticosterone (CORT) in the serum, the inflammatory cytokines in the liquid supernatant of the ileum and hippocampal homogenate, and apoptosis-regulated proteins in the liquid supernatant of hippocampal homogenate were measured by the commercial enzyme-linked immunosorbent assay (ELISA) kit for mice according to the manufacturer's instructions. The inflammatory cytokines included tumor necrosis factor-alpha (TNF-α), interleukin-1β (IL-1β), IL-6, interferon-gamma (IFN-γ), and IL-10 (only detects ileal tissue). All the commercial ELISA reagent kits were obtained from Enzyme-linked Biotechnology Company (Shanghai Enzyme-linked Biotechnology Co., Ltd., China).

2.6. Real-time quantitative polymerase chain reaction (qPCR) analysis of gene expression

The left hippocampus and partial ileal tissue were removed and washed with ice-cold sterilized saline without RNA enzyme (RNase) and then immediately frozen in liquid nitrogen for gene expression analysis. Total hippocampal RNA and ileal RNA were isolated using E.Z.N.A.® Total RNA Kit (OMEGA Bio-Tek) according to the manufacturer's instructions. Isolated RNA was assessed from the ratio of absorbance at 260/280 nm and agarose gel electrophoresis for quantitative and qualitative analyses. The isolated RNA was transcribed into first-strand complementary DNA with PrimeScript RT reagent kit with gDNA Eraser (Thermo Scientific, Waltham, Massachusetts, USA) according to the manufacturer's instructions. qPCR was performed with SYBR green and primers (details previously published) (Xin et al., 2014). The PCR conditions were as follows: 1 cycle at 95 °C for 5 min, followed by 40 cycles at 95 °C (10 s) and optimum temperature (30 s), and then a final melting curve analysis to monitor the purity of the PCR product. The optimum temperature of each gene was shown in Table A.3. β-Actin was used as reference genes to normalize the relative mRNA expression levels of target genes with values presented as $2^{-\Delta\Delta Cq}$. Primer sequences and optimum annealing temperatures were shown in Table A.3. The relative expression levels of neurogenesis-related factors [BDNF, CREB, stem cell factor (SCF), and neural cell adhesion molecule (NCAM)], molecular myelin structure [myelin oligodendrocyte glycoprotein (MOG), proteolipid protein (PLP), myelin basic protein (MBP), and myelin-associated glycoprotein (MAG)], apoptosis-related proteins [Bcl2-associated X protein (Bax), Bcl-xL/Bcl-2 asociated death promoter (Bad), B-cell lymphoma-2 (Bcl-2), B-cell lymphoma-extra large (Bcl-xl), caspase9, and caspase3), cytokines [interferon-γ (IFN-γ), tumor necrosis factor-α (TNF-α), interleukin (IL)-1β, IL-6, and IL-10] in the hippocampus, and tight junction (TJ) proteins [zonula occludens protein 1 (ZO-1), claudin-1, and occludin) in ileal tissue were detected.

2.7. Immunohistochemistry

Another four mice (one mouse per cage) in each group were sacrificed following exposure to 1 h WAS, and their brain and ileum were removed, fixed in 4% paraformaldehyde solution, and stored in 4 °C for immunohistochemical assay. Tissues were embedded by paraffin and cut by a microtome. Slices were submerged in citrate antigen retrieval solution and heated at medium heat until boiling using a microwave oven (model: P70D20TL-P4; Galanz, Guangdong, China). The temperature was ceased, and the tissues were kept warm for 8 min. Then, the tissues were heated at medium–low heat for 7 min. After free cooling, the slices were placed into PBS (pH 7.4) and shaken for 5 min for decoloration, which was repeated three times. Afterward, the sections were incubated in 3% oxydol for 25 min at room temperature and away from the light to block endogenous peroxidase. The slices were washed three times in PBS by shaking for 5 min, then sealed for 30 min by 3% bull serum albumin, and incubated with monoclonal rabbit anti-BDNF (1:400), polyclonal rabbit anti-CREB (1:500), anti-Occludin, anti-Claudin-1, or anti-ZO-1 (1:200) antibodies at 4 °C overnight. Species-specific biotinylated anti-rabbit immunoglobulin (horseradish peroxidase labeled) was used for immunodetection. Following the second antibody incubation, the 3,3′-diaminobenzidine staining kit was used to complete the reaction according to the manufacturer's instructions. Hematoxylin staining was performed to re-stain the nucleus.

2.8. 16S rRNA gene sequencing

The ileal content of the abovementioned mice and another ten mice (one mouse per cage) from each group without acute stress was collected and selected enough eight samples for 16S rRNA gene sequencing.

Bacterial genomic DNA was extracted using the E.Z.N.A.TM stool DNA isolation kit (Omega Bio-Tek, Doraville, CA). The final elution volume was 100 μL, and the integrity, purity, fragment size, and concentration were determined by electrophoresis with 1% agarose gel. The 16S V3-V4 was amplified by PCR using the primer 515F/806R of the 16SrRNA gene. Then, the purified PCR products were formed into a library with Ion Plus Fragment Library Kit 48 rxns (Thermofisher, USA) and sequenced in the Ion S5™XL platform (Thermofisher, USA) using the single-end sequencing. The primer contained adapter sequences and single-end barcodes, allowing pooling and direct sequencing of PCR products. Cutadapt (V1.9.1, http://cutadapt.readthedocs.io/en/stable/) was applied to the resulting high-quality 16SrRNA gene reads. The 16S rRNA gene read pairs were demultiplexed based on the unique molecular barcodes, and reads were merged using VSEARCH (Rognes et al., 2016). Sequences were clustered into operational taxonomic units (OTUs) at a similarity cutoff value of 97%. Then, OTU representative sequences were produced using the Uparse v7.0.1001. Species annotation analysis was performed on the OTU representative sequences through the SILVA Database. Homogenized data of each sample were constructed using the sample with the least amount of data as the standard. This sample was used for downstream analyses of alpha-diversity, beta-diversity, phylogenetic trends, and functional prediction.

3. Statistical analysis

The 16S rRNA sequencing data were analyzed by Wilcoxon rank-sum test to detect significant differences among the different groups.

All other results were reported by mean ± standard deviation. Normality was evaluated using the Shapiro-Wilk normality test. If data were not normally distributed they were log transformed for analysis. Data that remained not normally distributed were analyzed by Kruskal-Wallis test followed by Wilcoxon rank-sum test. If data were normally distributed they were analyzed by one-way analysis of variance (ANOVA) followed by post hoc Duncan's multiple range test. In short, All biochemical parameters were assessed by one-way ANOVA followed by post hoc Duncan's multiple range test except for BDNF using Kruskal-Wallis test followed by Wilcoxon rank-sum test. Differences of $p < 0.05$ were considered statistically significant. Data were analyzed with IBM SPSS Statistics 25.

4. Results

4.1. L. johnsonii BS15 improved the memory ability and serum CORT level in fluoride-treated mice exposed to WAS

As shown in Fig. 1A and B, the spontaneous exploration in the T-maze test and the exploration ratio in the NOR test were significantly reduced in the F group compared with the control and prob groups (T-maze: control vs. F, $P < 0.001$; F vs. prob, $P = 0.008$; NOR test: control vs. F, $P < 0.001$; F vs. prob, $P = 0.001$). No significant difference was

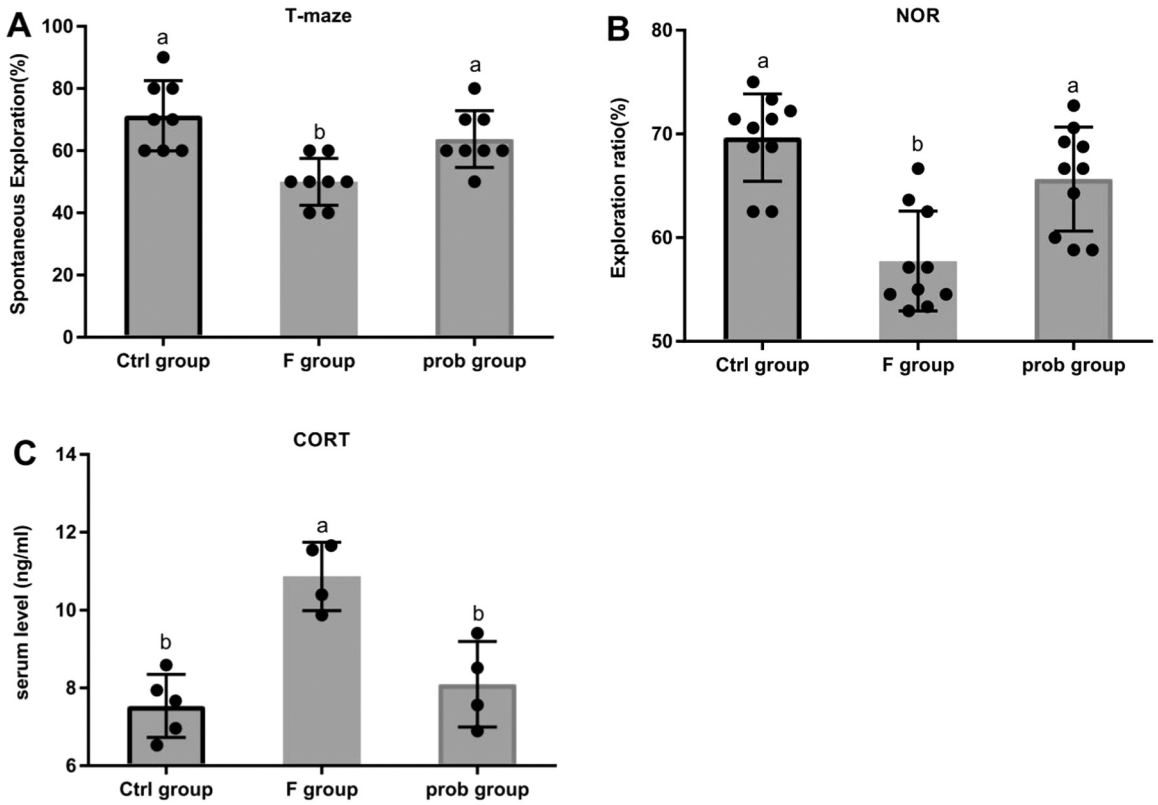

Fig. 1. Results of behavioral tests and the serum CORT level. (A) T-Maze (n = 8; one-way ANOVA, $F_{2,\ 21} = 10.407$, $P = 0.001$), (B) NOR preference tests (n = 10; one-way ANOVA, $F_{2,\ 27} = 16.685$, $P < 0.001$), and (C) the serum CORT level (n = 4–5; one-way ANOVA, $F_{2,\ 10} = 15.748$, $P = 0.001$). Data are presented as the means ± standard deviation. Bars with different letters indicate significant difference based on Duncan's multiple range test ($P < 0.05$).

observed in the abovementioned indexes between the control and prob groups (T-maze: $P = 0.127$; NOR test: $P = 0.068$). Fig. 1C shows that the F group exhibited a remarkably higher serum CORT level than the other two groups (control vs. F, $P < 0.001$; F vs. prob, $P = 0.002$), but no significant difference was found between the other two groups.

4.2. Effect of L. johnsonii BS15 on BDNF, CREB, NCAM, and SCF expressions in the hippocampus of fluoride-treated mice

Fig. 2A and B shows a sharp decrease in mRNA expression levels of BDNF (control vs. F, $P = 0.011$; F vs. prob, $P = 0.011$) and CREB (control vs. F, $P = 0.026$; F vs. prob, $P = 0.011$) in the F group compared with the other two groups. The mRNA level of BDNF in the control group was higher than that in the prob group ($P = 0.036$) (Fig. 2A). No difference was observed in the CREB mRNA level between the control and prob groups ($P = 0.448$) (Fig. 2B). Moreover, no significant difference in the NCAM was found among the three groups (control vs. F, $P = 0.058$; F vs. prob, $P = 0.058$; control vs. prob, $P = 0.058$) (Fig. 2C). Compared with the control group, the SCF mRNA level was remarkably reduced in the F group and slightly decreased in the prob group (control vs. F, $P = 0.005$; control vs. prob, $P = 0.062$) (Fig. 2D). By contrast, the prob group presented a slightly higher SCF mRNA level than the F group ($P = 0.164$) (Fig. 2D). As shown in Fig. 2E–J, the protein expression levels of BDNF and CREB were significantly reduced in the F group compared with that in the other two groups.

4.3. L. johnsonii BS15 alleviated the myelin damage and improved the apoptosis-related proteins in fluoride-treated mice exposed to WAS

Fig. 3A shows that the mRNA expression levels of PLP (control vs. F, $P < 0.001$; control vs. prob, $P = 0.002$) and MOG (control vs. F, $P = 0.007$; control vs. prob, $P = 0.005$) in the F and prob groups were sharply decreased compared with that in the control group. The PLP in the prob group was slightly higher than that in the F group ($P = 0.125$). No significant difference in the MOG was observed between the F and prob groups ($P = 0.994$). No changes in the MBP mRNA expression level were observed among the three groups (control vs. F, $P = 0.594$; control vs. prob, $P = 0.278$; F vs. prob, $P = 0.609$). As shown in Fig. 3A, the F group presented a significantly lower MAG mRNA level than the other two groups (control vs. F, $P < 0.001$; F vs. prob, $P < 0.001$). Compared with the control group, MAG was remarkably reduced in the prob group ($P = 0.01$).

No significant difference in the Bcl-2 mRNA level was found among the three groups (control vs. F, $P = 0.637$; control vs. prob, $P = 0.113$; F vs. prob, $P = 0.052$), whereas the prob group showed the highest among the three groups (Fig. 3B). In Fig. 3B, the F group presented a lower Bcl-xl mRNA level than the other two groups (control vs. F, $P = 0.042$; F vs. prob, $P = 0.021$), but no difference was observed in the other two groups (control vs. prob, $P = 0.8$). As shown in Fig. 3B, the Bax mRNA level in the F group was slightly increased compared with that in the other two groups, but no significant difference was observed among the three groups (control vs. F, $P = 0.734$; control vs. prob, $P = 0.772$; F vs. prob, $P = 0.531$). Fig. 3B shows a remarkably increased Bad mRNA level in the F group compared with the other two groups (control vs. F, $P = 0.047$; F vs. prob, $P = 0.012$), whereas no difference was observed in the other two groups (control vs. prob, $P = 0.445$). As shown in Fig. 3B, no significant difference in the caspase3 and caspase9 mRNA level was observed among the three groups (casepase3: control vs. F, $P = 0.139$; control vs. prob, $P = 0.195$; F vs. prob, $P = 0.902$; casepase9: control vs. F, $P = 0.256$; control vs. prob, $P = 0.476$; F vs. prob, $P = 0.62$), but caspase3 in the control group and caspase9 in the F group were the lowest and highest, respectively, among the three groups.

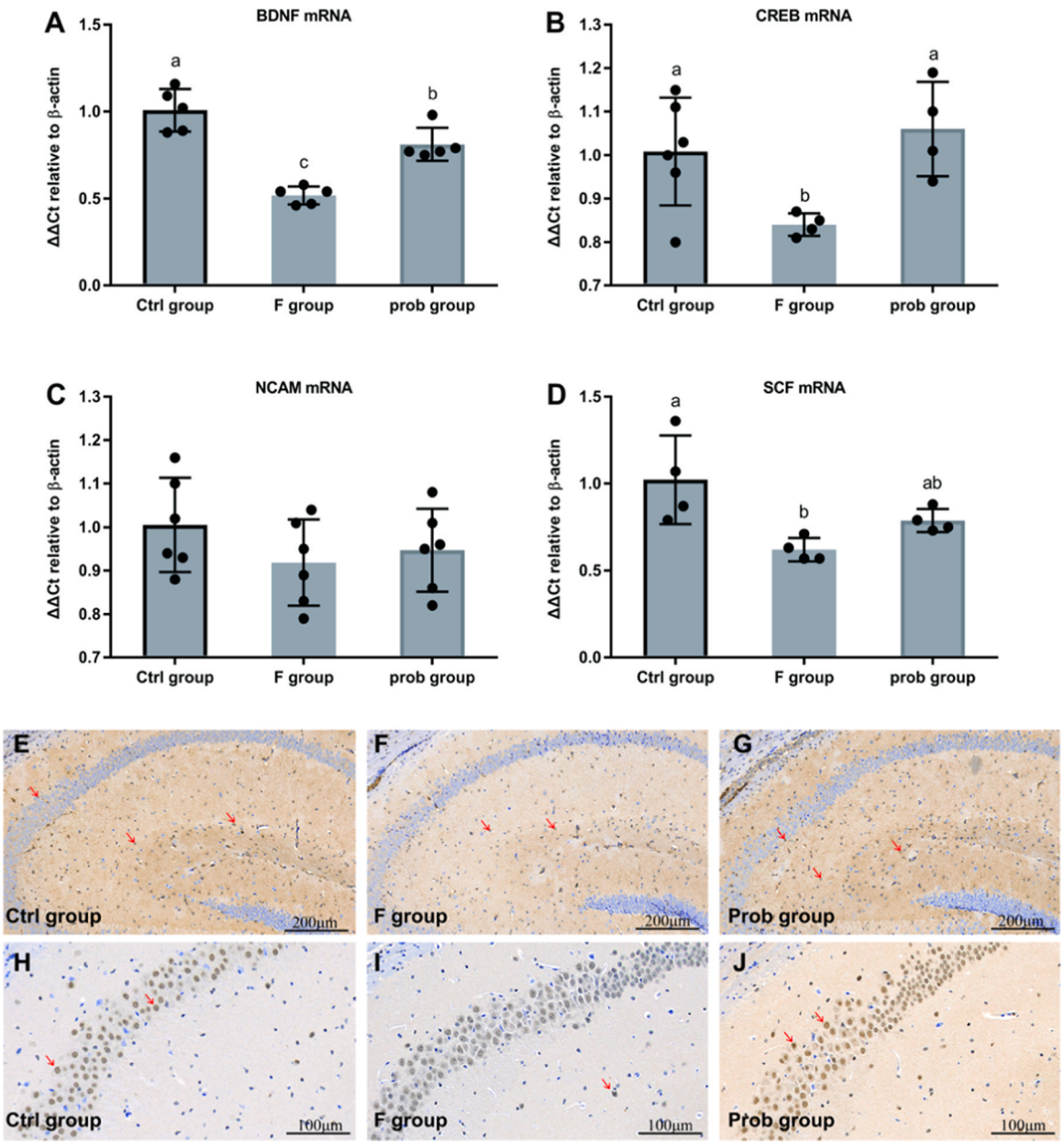

Fig. 2. Expressions of neurogenesis-related factors in the hippocampus. Relative expression levels of (A) BDNF (Kruskal–Wallis test, $H_2 = 11.622$, $P = 0.003$; Wilcoxon test, control vs. F, $P = 0.011$; F vs. prob, $P = 0.011$; control vs. prob, $P = 0.036$), (B) CREB (one-way ANOVA, $F_{2,\ 11} = 5.229$, $P = 0.025$), (C) NCAM (one-way ANOVA, $F_{2,\ 15} = 1.144$, $P = 0.345$), and (D) SCF (one-way ANOVA, $F_{2,\ 9} = 6.691$, $P = 0.017$). Immunohistochemistry of BDNF (E-G) and CREB (H-J) expression in the hippocampus of mice. The BDNF- and CREB-positive cells are brown like the arrow indication. Data are presented as the means ± standard deviation (n = 4–6). Bars with different letters indicate significant difference on the basis of Duncan's multiple range test (CREB, NCAM, SCF) or Wilcoxon test (BDNF) ($P < 0.05$). (For interpretation of the references to colour in this figure legend, the reader is referred to the web version of this article.)

4.4. L. johnsonii BS15 reduced the intestinal permeability in fluoride-treated mice exposed to WAS

As shown in Fig. 4A, the F group shows a markedly lower ZO-1 mRNA level than the other two groups (control vs. F, $P = 0.001$; F vs. prob, $P = 0.028$), but significant difference was not observed in the other two groups (control vs. prob, $P = 0.059$). Compared with the control group, the mRNA expression levels of claudin-1 (control vs. F, $P = 0.025$; control vs. prob, $P = 0.032$) and occludin (control vs. F, $P < 0.001$; control vs. prob, $P = 0.002$) were sharply decreased in the F and prob groups. No significant difference was observed in claudin-1 mRNA level between the F and prob groups ($P = 0.878$). The occludin mRNA level in the prob group was slightly higher than that in the F group ($P = 0.241$). The protein expressions of TJs were also detected by immunohistochemistry, and the results showed the same trend (Fig. 4C).

As shown in Fig. 4B, compared with the control group, the serum DAO content was significantly and slightly increased in the F and prob groups (control vs. F, $P = 0.021$; control vs. prob, $P = 0.182$), respectively. The control group showed a remarkably lower serum D-lactate activity than the other two groups (control vs. F, $P < 0.001$; control vs. prob, $P = 0.016$). By contrast, the D-lactate activity in the F group was significantly higher ($P = 0.018$) than that in the prob group.

4.5. L. johnsonii BS15 prevented disorder in the gut microbiota induced by fluoride

The gut microbiota with or without stress were observed in each group to determine the influence of fluoride and acute stress on the gut

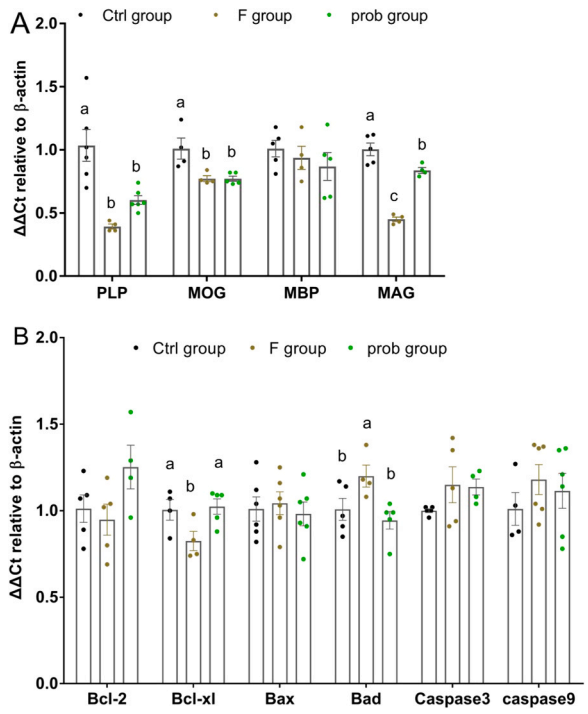

Fig. 3. mRNA expression levels of myelin- and apoptosis-associated proteins in the hippocampus. Relative expression levels of (A) PLP (one-way ANOVA, $F_{2,\ 13} = 13.906$, $P = 0.001$), MOG (one-way ANOVA, $F_{2,\ 10} = 8.091$, $P = 0.008$), MBP (one-way ANOVA, $F_{2,\ 11} = 0.651$, $P = 0.541$), and MAG (one-way ANOVA, $F_{2,\ 10} = 56.933$, $P < 0.001$). Relative expression levels of (B) Bcl-2 (one-way ANOVA, $F_{2,\ 11} = 2.559$, $P < 0.112$), Bcl-xl (one-way ANOVA, $F_{2,\ 10} = 4.269$, $P = 0.046$), Bax (one-way ANOVA, $F_{2,\ 15} = 0.206$, $P = 0.816$), Bad (one-way ANOVA, $F_{2,\ 11} = 4.704$, $P = 0.033$), caspase-3 (one-way ANOVA, $F_{2,\ 11} = 1.528$, $P = 0.260$), and caspase-9 (one-way ANOVA, $F_{2,\ 13} = 0.705$, $P = 0.512$). Data are presented as mean ± standard deviation (n = 4–6). Bars with different letters indicate significant difference on the basis of Duncan's multiple range test ($p < 0.05$).

microbiota. Through 16s rRNA gene sequencing, we did not find significant alterations in the gut microbiota of mice exposed to WAS versus non-stressed animals (Fig. 5A-C and Table A.4). Thus, the data with or without WAS were combined in each group.

As shown in Fig. 5D and Fig. A.2A, principal coordinate analysis (PCOA) based on unweighted UniFrac distances and principal component analysis (PCA) showed a clear separation between the ileal microbiota of mice in the F group and those in the other groups, whereas no significant separation was observed between the other two groups. Moreover, the observed species (Fig. 5E) and Shannon index (Fig. 5F) in the ileal lumen microbiome of mice in the F group were significantly increased compared with that in the control group, whereas significant increases were not observed in the prob group. The ileal microbial communities among the three groups were dominated by *Firmicutes* in the phylum level (Fig. 5G). Relative abundance of *Firmicutes* in the F group was significantly reduced compared with that in the control and prob groups (Fig. 5G and Fig. A.2B). On the contrary, the relative abundances of *Actinobacteria* (Fig. A.2C), *Bacteroidetes* (Fig. A.2D), and *Cyanobacteria* (Fig. A.2E) increased markedly in the F group compared with the control and prob groups. The alteration of these common phyla induced by fluoride was significantly inhibited by L. *johnsonii* BS15. At the genus level (Fig. 5H), *Lactobacillus* was the important bacterium in the control, F, and prob groups, and the relative abundance of the nine main genera found in the three groups was different. As shown in Fig. A.2F–N, the F group presented a sharply reduced relative abundance of *Lactobacillus* and *Candidatus_Arthromitus* and a significantly increased relative abundance of *Streptococcus*, *Romboutsia*, *Allobaculum*, *unidentified_Clostridiales*, *Dubosiella*, *Bifidobacterium*, and *unidentified_Lachnospiraceae* compared with the control group. However, L. *johnsonii* BS15 suppressed these alterations except for *Streptococcus*, *unidentified_Clostridiales*, *Bifidobacterium*, and *Candidatus_Arthromitus*. Compared with the control group, more genera bloomed or diminished in the ileal lumen of the F group than those in the prob group (Fig. 5I). Moreover, compared with the control group, multiple microbial pathways were altered in the F group, which were reversed in the prob group (Fig. 5J). As shown in Fig. 5K, PCA showed significant separation between the control and F groups in the function of the microbiome in KEGG pathways but was not observed between the control and prob groups.

4.6. Changes of dominant bacteria genus and correlation between bacteria and clinical data

As shown in Fig. 6A and B, compared with control and F groups, the significant discriminative taxa in the control group were *Firmicutes*, *Bacilli*, *Lactobacillales*, *Lactobacillaceae*, *Lactobacillus*, *Lactobacillus_taiwanensis*, *Lactobacillus_reuteri*, *Lactobacillus_intestinalis*, and in F group were *Clostridia*, *Erysipelotrichia*, *Clostridiales*, *Erysipelotrichales*, *Peptostreptococcaceae*, *Erysipelotrichaceae*, *Streptococcaceae*, *unidentified_Clostridiales*, *Lachnospiraceae*, *Romboutsia*, *Streptococcus*, *Allobaculum*, *Streptococcus_hyointestinalis*, *Streptococcus_hyointestinalis*. Compared with F and prob groups, the significant discriminative taxa in F group were *Erysipelotrichia*, *Clostridia*, *Erysipelotrichales*, *Clostridiales*, *unidentified_Clostridiales*, *Lachnospiraceae*, *Erysipelotrichaceae*, *Erysipelotrichaceae*, *unidentified_Lachnospiraceae*, *Dubosiella*, *unidentified_Clostridiales*, *Allobaculum*, *Romboutsia*, as well as *Clostridium_sp*_ND2, and in prob group were *Bacilli*, *Lactobacillales*, *Lactobacillaceae*, *Lactobacillus* (Fig. 6C and D). Compared with control and prob groups, the key genera in prob group were *Streptococcaceae*, *Streptococcus*, *Allobaculum*, *unidentified_Clostridiales*, *Streptococcus_hyointestinalis*, as well as *Clostridium_sp*_ND2, and in control group were *Lactobacillus_taiwanensis*, *Lactobacillus_reuteri*, *Lactobacillus_intestinalis* (Fig. 6E and F).

Fig. 7A shows that bacteria from phylum (Firmicutes, Actinbacteria, Bacteroidetes, Cyanobacteria) and genus (Lactobacillus, Streptococcus, Romboutsia, Allobaculum, unidentified_Clostridiales, Dubosiella, Bifidobacterium, unidentified_Lachnospiraceae, Candidatus_Arthromitus) in top ten level with significant difference among groups displayed significant associations with spontaneous exploration (T-maze), exploration ratio (NOR test), mRNA levels of BDNF, CREB, NCAM, and SCF of hippocampus except for Bifidobacterium. Firmicutes and Lactobacillus showed a positive regulation to these indexes. Fig. 7B shows that Cyanobacteria, Streptococcus, and unidentified_Clostridiales were observably positive associated with TNF-α and negative associated with IL-6. Moreover, IL-6 was also significantly and positively correlated with Lactobacillus and Candidatus_Arthromitus, and negatively correlated with unidentified_Lachnospiraceae. IFN-γ was significantly positively correlated with unidentified_Clostridiales and unidentified_Lachnospiraceae, and negatively correlated with Candidatus_Arthromitus. A significant association between myelin-associated protein, apoptosis-related proteins in hippocampus, and gut microbiota was not observed (Fig. 7C and D). Intestinal tight junction proteins were significantly associated with Cyanobacteria, Lactobacillus, and unidentified_Clostridiales (Fig. 7E).

5. Discussion

5.1. Behavioral phenotypes and neuroplasticity

A 70-day exposure to sodium fluoride was found to induce memory dysfunction in mice after 1 h exposure to WAS according to the results of behavioral tests in our present study. Lower memory ability was indicated by the low spontaneous exploration in T-maze test and low exploration ratio in NOR test in the fluoride-exposed group. Studies found that an hour of WAS exposure could not induce detectable

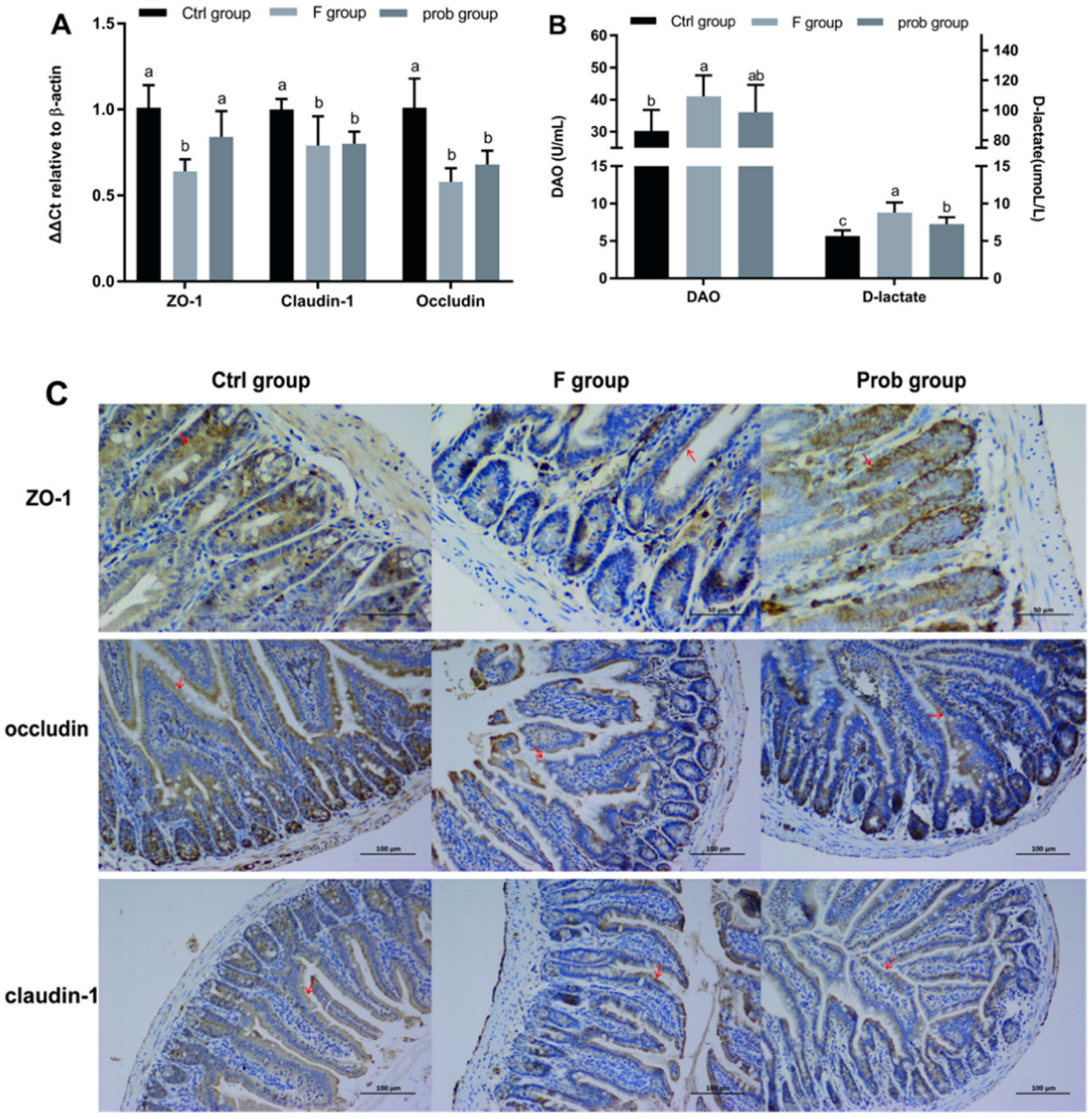

Fig. 4. Results of intestinal permeability. (A) mRNA expression levels of ZO-1 (one-way ANOVA, $F_{2,\ 10} = 11.689$, $P = 0.002$), claudin-1 (one-way ANOVA, $F_{2,\ 9} = 4.535$, $P = 0.043$) and occludin (one-way ANOVA, $F_{2,\ 11} = 16.702$, $P < 0.001$) in the ileum, (B) Serum DAO activity (one-way ANOVA, $F_{2,\ 15} = 3.333$, $P = 0.063$) and D-lactate concentration (one-way ANOVA, $F_{2,\ 15} = 14.382$, $P < 0.001$). (C) Immunohistochemistry of TJs protein expressions in ileum of mice. The ZO-1-, claudin-1- and occludin-positive cells are brown like the arrow indication. Data are presented as mean ± standard deviation (n = 4–6). Bars with different letters indicate significant difference on the basis of Duncan's multiple range test ($p < 0.05$). (For interpretation of the references to colour in this figure legend, the reader is referred to the web version of this article.)

behavioral changes in the T-maze and NOR tests but could cause a compounding effect on memory ability when combined with other stressors (e.g., endotoxin exposure and bacterial infection) by enhancing the HPA axis responsiveness (Gareau et al., 2011; Walker et al., 2008). We found that fluoride exposure resulted in HPA hyper-responsiveness to WAS given the significantly elevated CORT in the serum in F group. This result was consistent with that found by Gareau et al. (2011). Neuronal plasticity is the basis of learning and memory and occurs by neurogenesis, synaptic-dependent activity, cellular apoptosis, and reorganization of neuronal networks (Johnston, 2004, 2009). The hippocampus, a highly plastic region, is critical for learning and memory (Nakazawa et al., 2004). BDNF is one of the important modulators of neuroplasticity because of its multiple effects, such as increasing hippocampal neurogenesis, dendritic branching, cell proliferation, and promoting hippocampal long-term potentiation (Pang and Lu, 2004; Cassilhas et al., 2016). Blocking the hippocampal BDNF expression caused an impairment of spatial and reference memory (Mizuno et al., 2000). CREB, the transcriptional regulator of BDNF, has been considered as the central to AD pathology by similar genomic network analysis (Jeong et al., 2001). In addition, many studies using genetically modified mice revealed that a growing number of genes, such as CREB, BDNF, NCAM, and SCF, were involved in the regulation of neurogenesis. Consistent with our previous study Xin et al. (2020) and Niu et al. (2018), fluoride showed adverse effects on neuroplasticity as indicated by the remarkable decrease in the expressions of BDNF, CREB, and SCF on the mRNA and/or protein levels. Buffington et al. (2016) reported that the behavioral deficits and disordered gut microbiota in maternal high-fat diet offspring could be recovered by co-housing the offspring of mothers on a regular diet. Kumar et al. (2017) suggested that L. *johnsonii* could increase the concentrations of acetate and butyrate in feces. Butyrate, a short-chain fatty acid, could decrease BDNF methylation and consequently cause overexpression of BDNF by decreasing 10 to 11

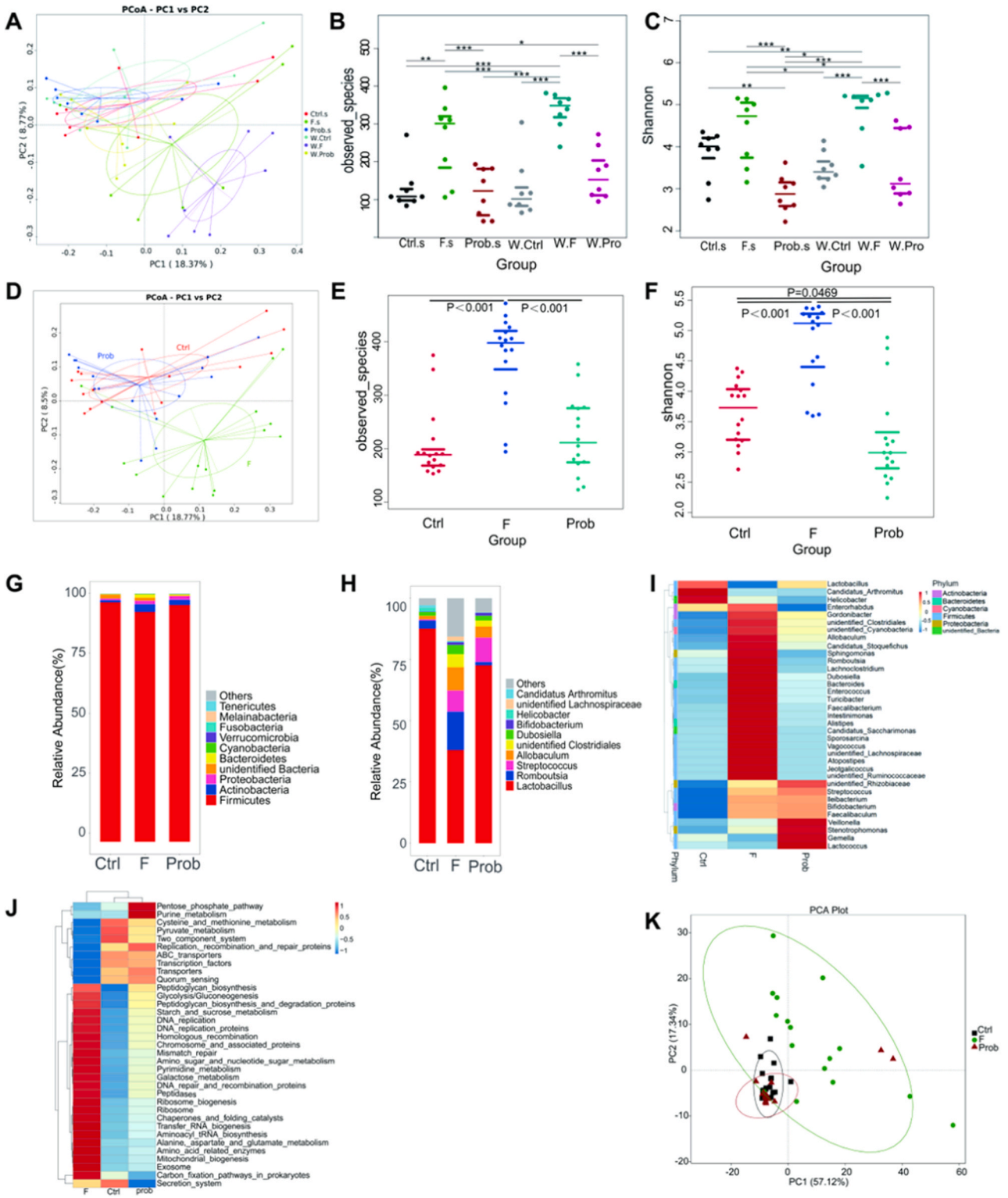

Fig. 5. Effects of L. *johnsonii* BS15 on the gut microbiome structure in fluoride-treated mice. (A) Principal coordinate analysis (PCoA) of unweighted UniFrac distances among groups with and without WAS. (B) Gut microbiome richness (observed species) in ileal luminal samples of each group. Significance: Wilcoxon. (C) Gut microbiome community diversity (Shannon) in each group. significance: Wilcoxon. (D) Principal coordinate analysis (PCoA) of unweighted UniFrac distances among the groups after combing data with and without WAS. (E) Gut microbiome richness (observed species) in ileal luminal samples of each group. Significance: Wilcoxon. (F) Gut microbiome community diversity (Shannon) in each group. Significance: Wilcoxon. (G) Relative abundance (%) at the phylum level of each group. (H) Relative abundance (%) at the genus level of each group. (I) Genera that are markedly altered by excess fluoride intake compared with the control group and reverted by L. *johnsonii* BS15. (J) Same as (I) but for KEGG pathways level 3. (K) Same as (A) PCA based on KEGG pathways level 3. Significance: Wilcoxon. $^{*}p < 0.05$, $^{**}p < 0.01$, $^{***}p < 0.001$. Ctrl.s: control group without WAS; F.s: F group without WAS; Prob.s: Prob group without WAS; W.Ctrl: control group with WAS; W.F: F group with WAS; W.Prob: Prob group with WAS.

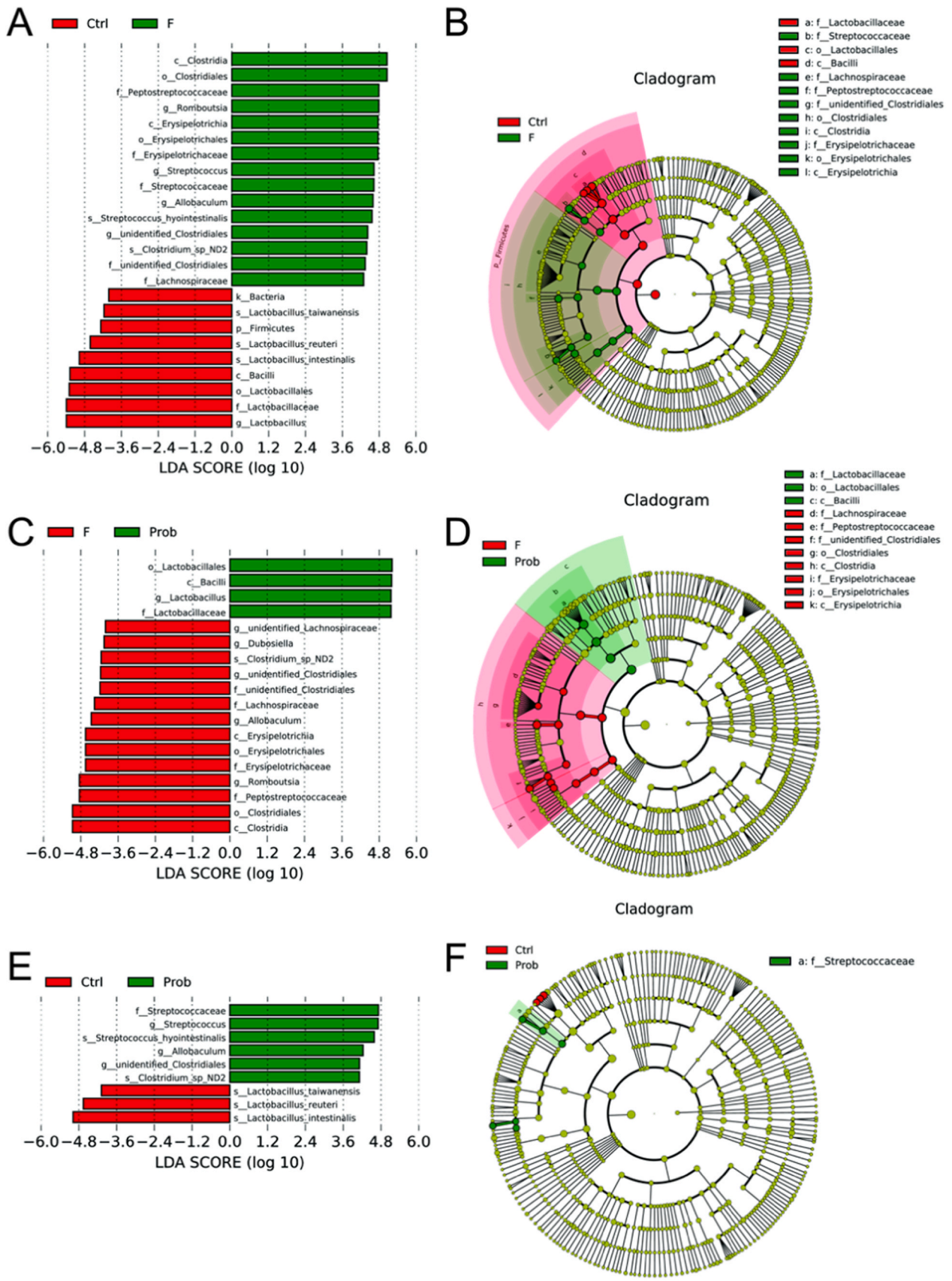

Fig. 6. LEfSe analysis of discriminative taxa of gut microbiota in mice. The linear discriminant analysis (LDA) score (A, C, and E) and cladogram (B, D, and F) were generated from LDA effect size (LEfSe). Only taxa meeting the LDA significance thresholds (> 4) are shown.

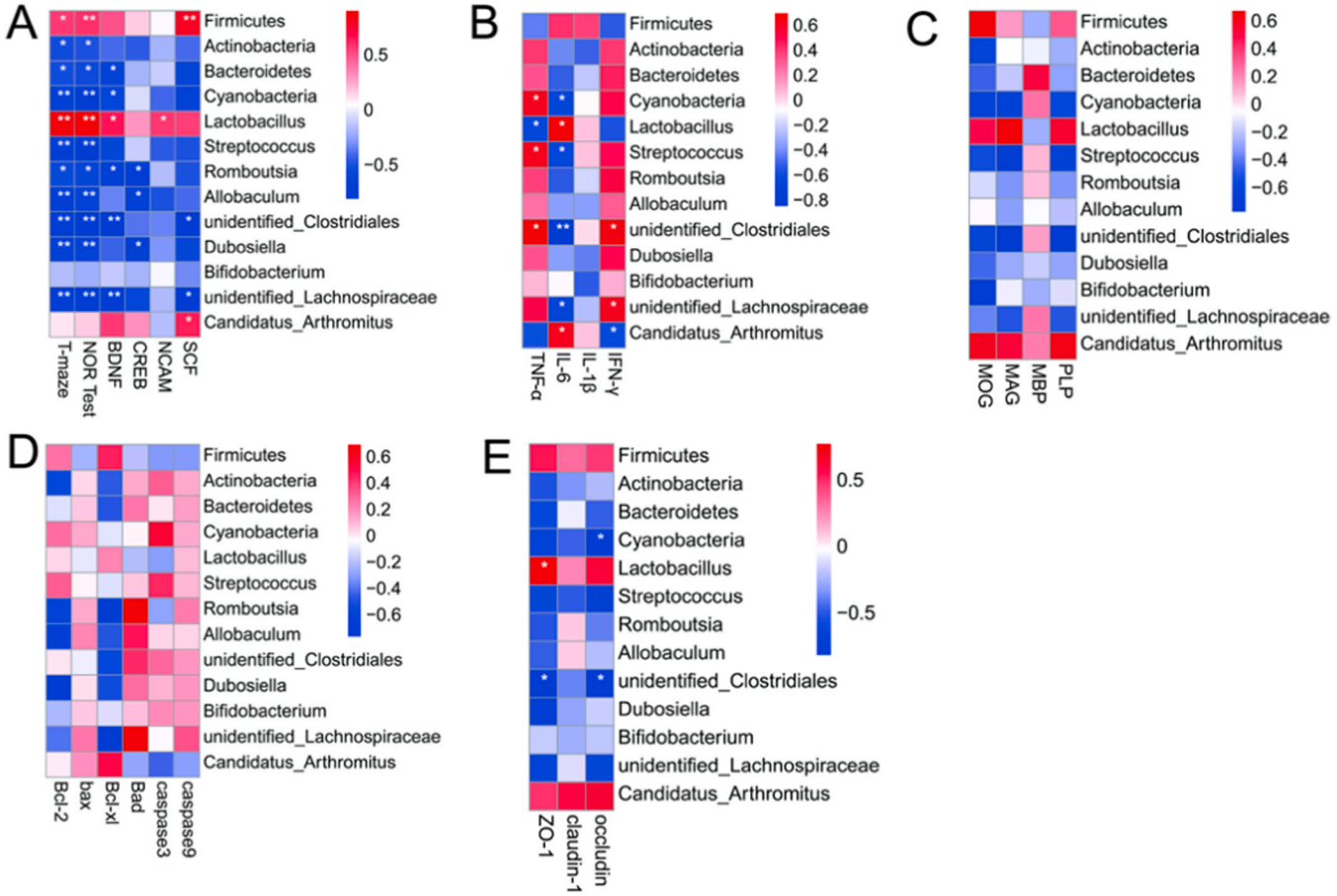

Fig. 7. Correlations analysis. (A) Correlations between intestinal flora and spontaneous exploration (T-maze), exploration ratio (NOR test), mRNA levels of BDNF, CREB, NCAM, and SCF of hippocampus. (B) Correlations between intestinal flora and protein expression levels of inflammatory cytokines in hippocampus. (C) Correlations between intestinal flora and mRNA expression levels of myelin-associated proteins of hippocampus. (D) Correlations between intestinal flora and apoptosis-related proteins of hippocampus. (E) Correlations between intestinal flora and intestinal tight junction proteins. The analysis method was spearman rank analysis. Bacteria were selected from phylum and genus in top ten level with significant difference. Heatmap showed that microbial taxa was positively or negatively related to behavioral phenotype and brain chemistry. $^{*}P < 0.05$ and $^{**}P < 0.01$ denoted statistical significance between bacterial taxa and biochemical parameters; Wilcoxon tests.

translocation methylcytosine dioxygenase 1, which was the enzyme responsible for catalyzing the conversion of DNA methylation to hydroxymethylation (Wei et al., 2014). Moreover, Luo et al. (2016) found that *Lactobacillus* spp. was significantly reduced in fluoride-treated broiler. Thus, in the present study, L. *johnsonii* BS15 was supplemented to fluoride-treated mice to investigate whether L. *johnsonii* BS15 could alleviate memory impairment. Based on our results, the L. *johnsonii* BS15-inoculated mice showed a significant memory improvement compared with fluoride-treated, stressed mice. Furthermore, the negative effects of fluoride treatment on the HPA response, BDNF, and CREB have been reversed by L. *johnsonii* BS15, indicating the psychoactive effect of the probiotic on memory impairment simultaneously induced by fluoride exposure and acute psychological stress.

5.2. Neuroinflammation, myelin-associated protein and neuron apoptosis

Chronic neuroinflammation attracts public attention for its role in mental health and diseases. However, considerable evidence proved that fluoride accumulation could activate microglia, a resident macrophage in the central nervous system (CNS), and lead to the production of proinflammatory cytokines. Prior studies have noted the importance of aberrant intestinal microbiota, altered intestinal immune response, and impaired intestinal barrier on neuroinflammation (Salehipour et al., 2017). In this study, we examined inflammatory cytokines in both mRNA and protein levels in the hippocampus to explore the influence of fluoride exposure on hippocampal inflammation in mice after WAS (Fig. A.3), which was consistent with our previous study (Xin et al., 2020). In addition, we observed the mRNA expression of myelin-associated protein to assess the effect of L. *johnsonii* BS15 on hippocampal impairment of fluoride-treated mice under psychological stress. Previous studies have demonstrated that fluoride could induce demyelination (Niu et al., 2018). In our previous study, we also found ten-week fluoride exposure induced significant decrease in PLP and MOG (Xin et al., 2020). After adding one hour WAS to fluoride-treated mice, not only the PLP and MOG, but also the decreased mRNA level of MAG was observed in this study. The down-regulated MAG induced by WAS in fluoride-treated mice was significantly increased by BS15 supplement. Notably, myelin sheath constituted by MOG, PLP, MBP, and MAG was important for axonal protection and interneuronal communication (Nguyen et al., 2009). MAG located in the innermost lamellae of myelin sheaths, as an inhibitor of mature axonal regeneration, could also promote stability and survival of myelinated axons (Nguyen et al., 2009). A local downregulation of MAG is the critical signal for CNS injury (Nguyen et al., 2009). Treatment with L. *johnsonii* BS15 effectively inhibited the reduction of MAG in fluoride-treated, stressed mice. Moreover, L. *johnsonii* BS15 upregulated the mRNA expression of Bcl-xl (anti-apoptotic) and downregulated the mRNA expression of Bad (pro-apoptotic) in the hippocampus of fluoride-treated and stressed mice, indicating that hippocampal apoptosis was linked to fluoride-induced memory impairment, whereas L. *johnsonii* BS15

improved hippocampal apoptosis.

5.3. Intestinal integrity

On the basis of recent reports, which associated bacteria and their products with memory in human (Emery et al., 2017; Zhan et al., 2016) (e.g., *E coli* K99, LPS), we focused on understanding the alterations of gut inflammation and intestinal integrity underlying the improvement of memory. We observed increased pro-inflammatory cytokines (TNF-α, IL-1β, and IFN-γ) and decreased anti-inflammatory cytokine (IL-10) which was in accordance with our previous study (Xin et al., 2020) (Fig. A.4). The improvement of BS15 on intestinal inflammation was also observed in fluoride-treated, stressed mice. TJ proteins (ZO-1, claudin-1, and occludin) in the mRNA and/or protein levels in the ileum of the F group were significantly reduced, indicating a damaged intestinal epithelial integrity. The increased serum DAO content and D-lactate activity in the fluoride-treated, stressed mice also indicated that fluoride increased gut permeability. Serum DAO activity and D-lactate content, indicators of mucosal integrity, would be increased when the intestinal mucosal integrity was destroyed (Luk et al., 1980; Ewaschuk et al., 2005). BS15 was detected to improve gut permeability of fluoride-treated mice under psychological stress according to the present results, which was consistent with the previous finding that specific probiotic administration could improve gut inflammation and intestinal mucosa integrity (Mujagic et al., 2017). Damaged intestinal mucosal integrity and some pro-inflammatory factors not only caused peripheral immune activation but also crossed the blood–brain barrier to aggravate neuroinflammation in the CNS under pathological conditions. Ait-Belgnaoui et al. (2012) also found that probiotic treatment could prevent leaky gut, thereby attenuating HPA response to acute psychological stress in rats. Hence, these results indicated that gut inflammation and intestinal mucosa integrity might be involved in the pathogenesis of neurotoxic effects of fluoride and might be the primary reason that BS15 improved memory deficit in fluoride-treated mice under acute stress.

5.4. The psychological stress

An hour of WAS exposure was added in this study to find whether or not the probiotic could alleviate fluoride-induced memory impairment after psychological stress through the gut-brain axis. Comparing to our previous work, several lines of evidence supported that WAS made the potential memory impairment more evident. It significantly aggravated the impact of fluoride exposure by influencing the gut-brain axis, which was most importantly supported by the result of NOR test in the present study. In this study, the exploration ratio was significantly lower in F group while it was not changed by single fluoride exposure in our previous work (Xin et al., 2020), directly indicating the impact of acute psychological stress in fluoride-treated mice. Apart from the behavioral phenotypes, differences between the changes of the expression levels of memory-associated and myelin-associated proteins in two studies also support the aggravation induced by WAS. Especially, the probiotic could not reverse the expression level of BDNF to baseline level in BS15-treated mice in the present study, and the expression level of SCF in fluoride-treated, stressed mice significant decreased in F group while no change was observed in our previous study (Xin et al., 2020). In addition, the improvement of BS15 on the reduced hippocampal PLP in fluoride-treated mice (Xin et al., 2020) was not observed in fluoride-treated, stressed mice according to the results in this study. We speculated that hyper-responsiveness to stress in fluoride-treated mice further inhibited the expression levels of these memory-associated proteins and thus make the potential memory impairment more evident in the present study. A previous study showed that repeated CORT injections reliably increased depression-like behavior on the forced-swim test in rats, suggesting that high levels of CORT contribute to the etiology of depression. Our hypothesis could therefore be supported by the comparison between the CORT results in two studies. We evaluated the CORT level in the serum in all three groups collected and stored in our previous work (Xin et al., 2020). Unlike the significantly higher level of CORT shown in F group in this study, no significant change of CORT level was observed according to the result we obtained (Fig. A.5). No significant change of claudin-1 was found in fluoride-treated mice without WAS (Xin et al., 2020), but the claudin-1 level was reduced in fluoride-treated, stressed mice in the present study. In addition, the probiotic did not show the same ability to reverse the decreased level of occludin in mice exposed by both fluoride and WAS as it was reported in the previous study (Xin et al., 2020). Therefore, based on the changes of tight junction proteins in this study, especially claudin-1 and occludin, an hour of WAS possibly aggravated the impact of fluoride intake on gut-brain axis and thus enhanced the memory impairment.

5.5. Gut microbiota

The gut microbiota is a key modulator of the bidirectional signaling pathways between the gut and brain. We conducted 16S rRNA gene sequencing on the ileal contents of mice to identify whether the reconstruction of gut microbiota was a potential mechanism underlying the hypothesis that BS15 protected mice from memory impairment induced by fluoride. According to the results shown in PCoA of unweighted UniFrac distances of microbiome communities structure before and after WAS and Table A.4, an hour of WAS exposure was not detected to significantly change the gut microbiota structure. We substantiated the composition differences of the gut microbiota in fluoride-treated mice through Adonis testing (Table A.5) and unweighted analyses of UniFrac distances, and the administration of L. *johnsonii* BS15 reversed those differences. *Firmicutes*, which accounted for up to 90% of the total sequences, was the dominant phylum in each group. Disordered gut microbiota in fluoride-exposed mice was primarily manifested by the relative abundance decrease of *Firmicutes* in the phylum level and *Lactobacillus* in the genus level. *Lactobacillus* is an important genus in *Firmicutes*. The relative abundance of *Lactobacillus* in the control, F, and prob groups was 87.7%, 38.1%, and 72.7%, respectively.The reduction of *Lactobacillus* induced by fluoride was consistent with the results of Luo et al. (2016).

Spearman correlation analysis in the genus level of the control group showed that *Lactobacillus* was negatively associated with most of the bacteria (66.7%; Fig. A.6A). In addition to the reduction of *Lactobacillus*, the above mentioned negative association between *Lactobacillus* and most bacteria was weakened and shifted to a positive association in the F group (Fig. A.6B), indicating that the inhibiting effect of *Lactobacillus* on other bacteria was weakened. The above observation also explains the increases in community diversity (Shannon index) and richness indices (number of observed features) in fluoride-treated mice. The administration of L. *johnsonii* BS15 reversed these changes (Fig. A.6C). This finding was in accordance with that of previous studies, which have suggested that *Lactobacillus* could suppress the growth of other bacteria, particularly harmful bacteria, because of its enzymatic, fibrinolytic, and broad-spectrum antimicrobial activity (Eom et al., 2015). New evidence by 16S rRNA gene sequencing of the gut microbial community in the genetically defined collaborative cross mouse cohort with different memory potentials showed that higher relative abundances of *Lactobacillus* indicated higher memory potential (Mao et al., 2020). This result was in accordance with that of Gareau et al. (2011), who showed that BDNF could reduce the risk of disorder and increase the stability of the gut microbiota. The function of the microbiome in KEGG pathways also mirrored the disorder induced by fluoride exposure and the reversion of L. *johnsonii* BS15.

The core genera in the control group compared with F group including *Firmicutes*, *Bacilli*, *Lactobacillales*, *Lactobacillaceae*, and *Lactobacillus* were health-associated bacterial communities, while most of core genera in F group were associated with disease (Griffen et al.,

2012). *Peptostreptococcaceae*, *Streptococcaceae*, and its genera *Streptococcus* were inflammation associated microbiota that are usually highly enriched in mice with intestinal inflammation (Xie et al., 2018). Increased *Clostridiales* was related to impaired memory potential (Magnusson et al., 2015). Mao et al. (2020) also reported improved memory is associated with higher relative abundances of *Lactobacillaceae* and lower relative abundances of *Clostridaceae*. *Clostridaceae* belong to *Clostridia*. BS15 reversed most of the discriminative taxa of mice exposed to fluoride. In this study, correlation analyses showed that core genera in F group including *unidentified_Clostridiales*, *Lachnospiraceae*, *Romboutsia*, *Streptococcus*, *Allobaculum* were significantly inversely correlated with memory potential and positively correlated with inflammatory reaction in hippocampus. *Lactobacillus*, the core genera in control and prob group compared to F group were significantly positively correlated with behavioral phenotype, nerve development related factors in this study, which is consistent with new evidence that higher relative abundances of *Lactobacillus* indicated higher memory potential (Mao et al., 2020). *Lactobacillus* was significantly anti-correlated with protein expression level of TNF-α which supported that it is a anti-inflammation-associated bacteria (Roychowdhury et al., 2018; Ait-Belgnaoui et al., 2014). Thus, the alteration of microbiota composition indicated that the reconstruction of the gut microbiota might be an important potential mechanism underlying the improvement of memory in BS15-inoculated mice.

6. Conclusion

This study showed that fluoride-exposed and stressed mice displayed impaired memory, damaged myelin, and a hyperactive HPA axis, coupled with a disordered gut microbiota structure particularly reduced relative abundance of *Lactobacillus*. Reconstruction of the gut microbiota by inoculating L. *johnsonii* BS15 could recover gut physiology, reverse memory deficit, alleviate myelin damage, and reduce the hyperactivity of the HPA axis. Collectively, our findings provided evidence to establish the link between gut microbiota reconstruction and gut-brain axis when using the probiotic to alleviate fluoride-induced memory impairment, and also proved the preventive effects of L. *johnsonii* BS15 on fluoride-induced memory impairment after psychological stress.

Funding

The present study was supported by Sichuan Science and Technology Program (2021YFH0097, 2019YHF0060).

CRediT authorship contribution statement

JX, HW, DZ, YB, and XN: Conceptualization, Methodology. **JX, NS, LL, and AK**: Project administration, Data curation, Writing - original draft. **YZ and KP**: Writing - original draft. **YW, HM, and SB**: Writing - review & editing. **BJ and XN**: Supervision.

Declaration of Competing Interest

The authors declare that they have no known competing financial interests or personal relationships that could have appeared to influence the work reported in this paper.

Acknowledgements

The authors gratefully acknowledge the help from Ms. Peng Xueji and Mr. Zhang Shuai for all the hard working during the behavioral tests, as well as Dr. Buriro Rehana and Danish Sharafat Rajput for the later revision of the article. Also, we really appreciate the supports provided by all other undergraduates during the animal feeding and sampling.

Appendix A. Supporting information

Supplementary data associated with this article can be found in the online version at doi:10.1016/j.ecoenv.2021.112108.

References

Ait-Belgnaoui, A., Durand, H., Cartier, C., Chaumaz, G., Eutamene, H., Ferrier, L., Houdeau, E., Fioramonti, J., Bueno, L., Theodorou, V., 2012. Prevention of gut leakiness by a probiotic treatment leads to attenuated HPA response to an acute psychological stress in rats. Psychoneuroendocrinology 37, 1885–1895. https://doi.org/10.1016/j.psyneuen.2012.03.024.

Ait-Belgnaoui, A., Colom, A., Braniste, V., Ramalho, L., Marrot, A., Cartier, C., Houdeau, E., Theodorou, V., Tompkins, T., 2014. Probiotic gut effect prevents the chronic psychological stress-induced brain activity abnormality in mice. Neurogastroenterol. Motil. 26, 510–520. https://doi.org/10.1111/nmo.12295. Epub 2013 Dec 30.

Antunes, M., Biala, G., 2012. The novel object recognition memory: neurobiology, test procedure, and its modifications. Cogn. Process. 13, 93–110. https://doi.org/10.1007/s10339-011-0430-z.

Bashash, M., Thomas, D., Hu, H., Martinez-Mier, E.A., Sanchez, B.N., Basu, N., Peterson, K.E., Ettinger, A.S., Wright, R., Zhang, Z., Liu, Y., Schnaas, L., Mercado-García, A., Téllez-Rojo, M.M., Hernández-Avila, M., 2017. Prenatal fluoride exposure and cognitive outcomes in children at 4 and 6-12 years of age in Mexico. Environ. Health Perspect. 125, 097017 https://doi.org/10.1289/EHP655.

Buffington, S.A., Prisco, G.V., Auchtung, T.A., Ajami, N.J., Petrosino, J.F., Costa-Mattioli, M., 2016. Microbial reconstitution reverses maternal diet-induced social and synaptic deficits in offspring. Cell 165, 1762–1775. https://doi.org/10.1016/j.cell.2016.06.001.

Cassilhas, R.C., Tufik, S., Mello, M.T., 2016. Physical exercise, neuroplasticity, spatial learning and memory. Cell. Mol. Life Sci. 73, 975–983. https://doi.org/10.1007/s00018-015-2102-0.

Coryell, M., McAlpine, M., Pinkham, N.V., McDermott, T.R., Walk, S.T., 2018. The gut microbiome is required for full protection against acute arsenic toxicity in mouse models. Nat. Commun. 9, 5424. https://doi.org/10.1038/s41467-018-07803-9.

Deacon, R.M.J., Rawlins, J.N.P., 2006. T-maze alternation in the rodent. Nat. Protoc. 1, 7–12. https://doi.org/10.1038/nprot.2006.2.

Ding, Y., Gao, Y., Sun, H., Han, H., Wang, W., Ji, X., Liu, X., Sun, D., 2011. The relationships between low levels of urine fluoride on children's intelligence, dental fluorosis in endemic fluorosis areas in Hulunbuir, Inner Mongolia, China. J. Hazard Mater. 186, 1942–1946. https://doi.org/10.1016/j.jhazmat.2010.12.097.

Emery, D.C., Shoemark, D.K., Batstone, T.E., Waterfall, C.M., Coghill, J.A., Cerajewska, T.L., Davies, M., West, N.X., Allen, S.J., 2017. 16S rRNA next generation sequencing analysis shows bacteria in Alzheimer's post-mortem brain. Front. Aging Neurosci. 9, 195. https://doi.org/10.3389/fnagi.2017.00195.

Eom, J.S., Song, J., Choi, H.S., 2015. Protective effects of a novel probiotic strain of *Lactobacillus plantarum* JSA22 from traditional fermented soybean food against infection by salmonella enterica serovar typhimurium. J. Microbiol. Biotechnol. 25, 479–491. https://doi.org/10.4014/jmb.1501.01006.

Ewaschuk, J.B., Naylor, J.M., Zello, G.A., 2005. D-lactate in human and ruminant metabolism. J. Nutr. 135, 1619–1625. https://doi.org/10.1093/jn/135.7.1619.

Fein, N.J., Cerklewski, F.L., 2001. Fluoride content of foods made with mechanically separated chicken. J. Agr. Food Chem. 49, 4284–4286. https://doi.org/10.1021/jf0106300.

Fung, K.F., Zhang, Z.Q., Wong, J.W.C., Wong, M.H., 1999. Fluoride contents in tea and soil from tea plantations and the release of fluoride into tea liquor during infusion. Environ. Pollut. 104, 0–205. https://doi.org/10.1016/S0269-7491(98)00187-0.

Gareau, M.G., Wine, E., Rodrigues, D.M., Cho, J.H., Whary, M.T., Philpott, D.J., Macqueen, G., Sherman, P.M., 2011. Bacterial infection causes stress-induced memory dysfunction in mice. Gut 60, 307–317. https://doi.org/10.1136/gut.2009.202515.

Grandjean, P., 2019. Developmental fluoride neurotoxicity: an updated review. Environ. Health 18, 110. https://doi.org/10.1186/s12940-019-0551-x.

Grandjean, P., Landrigan, P.J., 2014. Neurobehavioural effects of developmental toxicity. Lancet Neurol. 13, 330–338. https://doi.org/10.1016/S1474-4422(13)70278-3.

Green, R., Lanphear, B., Hornung, R., Flora, D., Martinez-Mier, A., Neufeld, R., Ayotte, P., Muckle, G., Till, C., 2020. Fluoride exposure from infant formula and child IQ in a Canadian birth cohort. Environ. Int. 134, 105315 https://doi.org/10.1016/j.envint.2019.105315.

Griffen, A.L., Beall, C.J., Campbell, J.H., Firestone, N.D., Kumar, P.S., Yang, Z.K., Podar, M., Leys, E.J., 2012. Distinct and complex bacterial profiles in human periodontitis and health revealed by 16S pyrosequencing. ISME J. 6, 1176–1185. https://doi.org/10.1038/ismej.2011.191.

Goulart, B.K., de Lima, M.N.M., de Farias, C.B., Reolon, G.K., Almeida, V.R., Quevedo, J., Kapczinski, F., Schröder, N., Roesler, R., 2010. Ketamine impairs recognition memory consolidation and prevents learning-induced increase in hippocampal brain-derived neurotrophic factor levels. Neuroscience 167, 969–973. https://doi.org/10.1016/j.neuroscience.2010.03.032.

Jang, S.E., Lim, S.M., Jeong, J.J., Jang, H.M., Lee, H.J., Han, M.J., Kim, D.H., 2018. Gastrointestinal inflammation by gut microbiota disturbance induces memory impairment in mice. Mucosal Immunol. 11, 369–379. https://doi.org/10.1038/mi.2017.49.

Jeong, H., Mason, S.P., Barabási, A.L., Oltvai, Z.N., 2001. Lethality and centrality in protein networks. Nature 411, 41–42. https://doi.org/10.1038/35075138.
Johnston, M.V., 2004. Clinical disorders of brain plasticity. Brain Dev. 26, 73–80. https://doi.org/10.1016/S0387-7604(03)00102-5.
Johnston, M.V., 2009. Plasticity in the developing brain: implications for rehabilitation. Dev. Disabil. Res. Rev. 15, 94–101. https://doi.org/10.1002/ddrr.64.
Kumar, S., Pattanaik, A.K., Sharma, S., Jadhav, S.E., Dutta, N., Kumar, A., 2017. Probiotic potential of a *Lactobacillus* bacterium of canine Faecal-Origin and its impact on ielect gut health indices and immune response of dogs. Probiotics Antimicrob. Proteins 9, 262–277. https://doi.org/10.1007/s12602-017-9256-z.
Liu, Y.J., Gao, Q., Wu, C.X., Guan, Z.Z., 2010. Alterations of nAChRs and ERK1/2 in the brains of rats with chronic fluorosis and their connections with the decreased capacity of learning and memory. Toxicol. Lett. 192, 324–329. https://doi.org/10.1016/j.toxlet.2009.11.002.
Luk, G.D., Bayless, T.M., Baylin, S.B., 1980. Diamine oxidase (histaminase). A circulating marker for rat intestinal mucosal maturation and integrity. J. Clin. Investig. 66, 66–70. https://doi.org/10.1172/JCI109836.
Luo, Q., Cui, H., Peng, X., Fang, J., Zuo, Z., Deng, J., Liu, J., Deng, Y., 2016. Dietary high fluorine alters intestinal microbiota in broiler chickens. Biol. Trace Elem. Res. 173, 483–491. https://doi.org/10.1007/s12011-016-0672-9.
Magnusson, K.R., Hauck, L., Jeffrey, B.M., Elias, V., Humphrey, A., Nath, R., Perrone, A., Bermudez, L.E., 2015. Relationships between diet-related changes in the gut microbiome and cognitive flexibility. Neuroscience 300, 128–140. https://doi.org/10.1016/j.neuroscience.2015.05.016.
Mao, J.H., Kim, Y.M., Zhou, Y.X., Hu, D., Zhong, C., Chang, H., Brislawn, C.J., Fansler, S., Langley, S., Wang, Y., Peisl, B.Y.L., Celniker, S.E., Threadgill, D.W., Wilmes, P., Orr, G., Metz, T.O., Jansson, J.K., Snijders, A.M., 2020. Genetic and metabolic links between the murine microbiome and memory. Microbiome 8, 53. https://doi.org/10.1186/s40168-020-00817-w.
Mizuno, M., Yamada, K., Olariu, A., Nawa, H., Nabeshima, T., 2000. Involvement of brain-derived neurotrophic factor in spatial memory formation and maintenance in a radial arm maze test in rats. J. Neurosci. 20, 7116–7121. https://doi.org/10.1523/JNEUROSCI.20-18-07116.2000.
Mujagic, Z., Vos, P., Boekschoten, M.V., Govers, C., Pieters, H.J., Wit, N.J.W., Bron, P.A., Masclee, A.A.M., Troos, F.J., 2017. The effects of *Lactobacillus plantarum* on small intestinal barrier function and mucosal gene transcription; a randomized double-blind placebo controlled trial. Sci. Rep. 7, 40128. https://doi.org/10.1038/srep40128.
Nakazawa, K., McHugh, T.J., Wilson, M.A., Tonegawa, S., 2004. Nmda receptors, place cells and hippocampal spatial memory. Nat. Rev. Neurosci. 5, 361–372. https://doi.org/10.1007/s10071-012-0495-9.
Neuendorf, R., Harding, A., Stello, N., Hanes, D., Wahbeh, H., 2016. Depression and anxiety in patients with inflammatory bowel disease: a systematic review. J. Psychosom. Res. 87, 70–80. https://doi.org/10.1016/j.jpsychores.2016.06.001.
Nguyen, T., Mehta, N.R., Conant, K., Kim, K.J., Jones, M., Calabresi, P.A., Melli, G., Hoke, A., Schnaar, R.L., Ming, G.L., Song, H., Keswani, S.C., Griffin, J.W., 2009. Axonal protective effects of the myelin-associated glycoprotein. J. Neurosci. 29, 630–637. https://doi.org/10.1523/JNEUROSCI.5204-08.2009.
Niu, R., Chen, H., Manthari 1, Ram Kumar, Sun 1, Zilong, Wang 1, Jinming, Zhang 1, Jianhai, Wang, Jundong, 2018. Effects of fluoride on synapse morphology and myelin damage in mouse hippocampus. Chemosphere 194, 628–633. https://doi.org/10.1016/j.chemosphere.2017.12.027.
Pang, P.T., Lu, B., 2004. Regulation of late-phase LTP and long-term memory in normal and aging hippocampus: role of secreted proteins tPA and BDNF. Ageing Res. Rev. 3, 407–430. https://doi.org/10.1016/j.arr.2004.07.002.
Petrone, P., Guarinob, F.M., Giustino, S., Gombos, F., 2013. Ancient and recent evidence of endemic fluorosis in the Naples Area. J. Geochem. Explor. 131, 14–27. https://doi.org/10.1016/j.gexplo.2012.11.012.
Qian, W., Miao, K., Li, T., Zhang, Z., 2013. Effect of selenium on fluoride-induced changes in synaptic plasticity in rat hippocampus. Biol. Trace Elem. Res. 155, 253–260. https://doi.org/10.1007/s12011-013-9773-x.
Rafique, T., Naseem, S., Ozsvath, D., Hussain, R., Bhanger, M.I., Usmani, T.H., 2015. Geochemical controls of high fluoride groundwater in Umarkot Sub-District, Thar Desert, Pakistan. Sci. Total Environ. 530–531, 271–278. https://doi.org/10.1016/j.scitotenv.2015.05.038.
Rognes, T., Flouri, T., Nichols, B., Quince, C., Mahé, F., 2016. VSEARCH: a versatile open source tool for metagenomics. PeerJ 4, e2584. https://doi.org/10.7717/peerj.2584.
Roychowdhury, S., Cadnum, J., Glueck, B., Obrenovich, M., Donskey, C., Cresci, G.A.M., 2018. Faecalibacterium prausnitzii and a prebiotic protect intestinal health in a mouse model of antibiotic and clostridium difficile exposure. JPEN 42, 1156–1167.
Salehipour, Z., Haghmorad, D., Sankian, M., Rastin, M., Nosratabadi, R., Dallal, M.M.S., Tabasi, N., Khazaee, M., Nasiraii, L.R., Mahmoudi, M., 2017. Bifidobacterium animalis in combination with human origin of *Lactobacillus plantarum* ameliorate neuroinflammation in experimental model of multiple sclerosis by altering CD4+ T cell subset balance. Biomed. Pharmacother. 95, 1535–1548. https://doi.org/10.1016/j.biopha.2017.08.117.
Srivastava, S., Flora, S.J.S., 2020. Fluoride in drinking water and skeletal fluorosis: a review of the global impact. Curr. Environ. Health Rep. 7, 140–146. https://doi.org/10.1007/s40572-020-00270-9.
Strandwitz, P., 2018. Neurotransmitter modulation by the gut microbiota. Brain Res. 1693, 128–133. https://doi.org/10.1016/j.brainres.2018.03.015.
Sun, D.J., 2010. Discussion on prevention and treatment strategies of endemic fluorosis in China. Chin. J. Endem. 29, 119–120. https://doi.org/10.3760/cma.j.issn.1000-4955.2010.02.001 (in Chinese).
Sun, Y.F., Zhao, L.J., Sun, D.J., 2009. Study on evaluation index and standard of the control in endemic fluorosis area. Chin. J. Endem. 28, 225–227. https://doi.org/10.3760/cma.j.issn.1000-4955.2009.02.033 (in Chinese).
Walker, F.R., Knott, B., Hodgson, D.M., 2008. Neonatal endotoxin exposure modifies the acoustic startle response and circulating levels of corticosterone in the adult rat but only following acute stress. J. Psychiatr. Res. 42, 1094–1103. https://doi.org/10.1016/j.jpsychires.2007.12.006.
Wang, H., Sun, Y., Xin, J., Zhang, T., Sun, N., Ni, X., Zeng, D., Bai, Y., 2020. *Lactobacillus johnsonii* BS15 prevents psychological stress–induced memory dysfunction in mice by modulating the gut–brain axis. Front. Microbiol. 11 https://doi.org/10.3389/fmicb.2020.01941.
Wei, Y., Melas, P.A., Wegener, G., Mathé, A.A., Lavebratt, C., 2014. Antidepressant-like effect of sodium butyrate is associated with an increase in TET1 and in 5-hydroxymethylation levels in the Bdnf gene. Int. J. Neuropsychopharmacol. 18, pyu032. https://doi.org/10.1093/ijnp/pyu032.
Wu, W., Sun, M., Zhang, H., Chen, T., Wu, R., Liu, C., Yang, G., Geng, X., Feng, B., Liu, Z., Yang, P., 2014. Prolactin mediates psychological stress-induced dysfunction of regulatory T cells to facilitate intestinal inflammation. Gut 63, 1883–1892. https://doi.org/10.1136/gutjnl-2013-306083.
Xie, R., Sun, Y., Wu, J., Huang, S., Jin, G., Guo, Z., Zhang, Y., Liu, T., Liu, X., Cao, X., Wang, B., Cao, H., 2018. Maternal high fat diet alters gut microbiota of offspring and exacerbates DSS-induced colitis in adulthood. Front. Immunol. 9, 2608. https://doi.org/10.3389/fimmu.2018.02608.
Xin, J., Zeng, D., Wang, H., Ni, X., Yi, D., Pan, K., Jing, B., 2014. Preventing non-alcoholic fatty liver disease through *Lactobacillus johnsonii* BS15 by attenuating inflammation and mitochondrial injury and improving gut environment in obese mice. Appl. Microbiol. Biotechnol. 98, 6817–6829. https://doi.org/10.1007/s00253-014-5752-1.
Xin, J., Zeng, D., Wang, H., Sun, N., Khalique, A., Zhao, Y., Wu, L., Pan, K., Jing, B., Ni, X., 2020. *Lactobacillus johnsonii* BS15 improves intestinal environment against fluoride-induced memory impairment in mice—a study based on the gut-brain axis hypothesis. PeerJ 8, e10125. https://doi.org/10.7717/peerj.10125.
Yan, X., Dong, N., Hao, X., Xing, Y., Tian, X., Feng, J., Xie, J., Lv, Y., Wei, C., Gao, Y., Qiu, Y., Wang, T., 2019. Comparative transcriptomics reveals the role of the toll-like receptor signaling pathway in fluoride-induced cardiotoxicity. J. Agric. Food Chem. 67, 5033–5042. https://doi.org/10.1021/acs.jafc.9b00312.
Zhan, X., Stamova, B., Jin, L.W., DeCarli, C., Phinney, B., Sharp, F.R., 2016. Gram-negative bacterial molecules associate with Alzheimer disease pathology. Neurology 87, 2324–2332. https://doi.org/10.1212/WNL.0000000000003391.
Zhao, B., Wu, J., Li, J., Bai, Y., Luo, Y., Ji, B., Xia, B., Liu, Z., Tan, X., Lv, J., Liu, X., 2020. Lycopene alleviates DSS-induced colitis and behavioral disorders via mediating microbes-gut-brain axis balance. J. Agric. Food Chem. 68, 3963–3975. https://doi.org/10.1021/acs.jafc.0c00196.